

# Use of Least Means Squares Filter in Control of Optical Beam Jitter

R. Joseph Watkins\*

*U.S. Naval Academy, Annapolis, Maryland 21402*

and

Brij N. Agrawal†

*Naval Postgraduate School, Monterey, California 93943*

DOI: 10.2514/1.26778

Meeting optical beam jitter requirements is becoming a challenging problem for several space programs. A laser beam jitter control test bed has been developed at the Naval Postgraduate School to develop improved jitter control techniques. Several control techniques, such as least means squares and linear–quadratic regulator were applied for jitter control. Enhancement in least means squares techniques to improve convergence rate was achieved by adding an adaptive bias filter to the reference signal. In the experiments, the platform is vibrated at 50 and 87 Hz. In addition, a fast steering mirror is used to inject a random component of 200 Hz band-limited white noise. The experimental results demonstrated that the addition of the adaptive bias filter to the least means squares algorithm significantly increased the converging rate of the controller. To achieve the reduction of both sinusoidal and random jitter, a combination of least means squares/adaptive bias filter and linear–quadratic regulator is most effective. The least means squares/adaptive bias filter control is most effective for a sinusoidal jitter and the linear–quadratic regulator control for a random jitter.

## Nomenclature

$A$	= cross-coupling factor	$\zeta$	= damping coefficient
$A, B, C, D$	= state–space matrices	$\theta$	= angle of mirror
$D_m$	= distance from source to mirror	$\phi$	= delay through a transfer function
$d$	= disturbance signal	$\omega_n$	= natural frequency, radians per second
$E$	= bias error	<i>subscripts</i>	
$E'$	= adaptive bias	$o$	= optical bench and mirrors
$e$	= error signal	$p$	= optical detector
$F$	= amplitude of sinusoidal disturbance	$s$	= fast steering mirror transfer function
$f$	= frequency, cycles per second	$w$	= adapting filter transfer function
$G$	= gain	$x$	= $x$ axis
$H$	= transfer function	$y$	= $y$ axis
$J$	= cost function		
$K$	= amplitude of reference signal		
$P$	= optical bench gain		
$Q, R$	= weighting matrices		
$S$	= fast steering mirror transfer function		
$s$	= Laplace variable		
$\hat{s}$	= estimate of fast steering mirror transfer function, finite impulse response coefficients		
$T$	= time constant		
$T_s$	= sample time		
$u$	= control signal or input		
$V$	= voltage		
$v$	= disturbance source		
$W$	= gain of adapting filter		
$w(n)$	= vector of tap gains		
$x$	= state vector		
$x(n)$	= reference signal		
$y$	= output vector		

## I. Introduction

MANY future space missions, laser communication systems, and imaging systems will require optical beam jitter control in the nanoradian regime [1]. Jitter is the undesired fluctuations in the pointing of an optical beam due to environmental or structural interactions, and consists of both broadband and narrowband disturbances. The narrow band jitter is generally created in a spacecraft by rotating devices such as reaction wheels, control moment gyros, cryocoolers and the motion of flexible structures, such as solar arrays. The effect of the atmosphere on the laser beam adds a broadband disturbance, when transmissions to or from the ground are considered. The control of jitter is currently a challenging problem for programs such as the James Webb Space Telescope, the U.S. Department of Defense Airborne Laser project, and any type of imaging spacecraft [2]. Jitter has a great effect on the resolution of an image or the intensity of an optical beam. For example, a 100 mm diam laser beam with 10  $\mu$ rad of jitter will result in roughly a 400-fold decrease in the intensity of the beam at 100 km, due to the jitter alone.

To achieve jitter control, several techniques have been proposed, including both classical and adaptive control systems. Several experimental setups have been used to test the viability of different control techniques. McEver and Clark used a linear–quadratic Gaussian (LQG) design to actively control jitter in an experiment designed around fast steering mirrors (FSM), accelerometers, and microphones [3]. The disturbance was acoustically induced by loudspeakers and control was attempted using feedforward from a

Received 25 July 2006; accepted for publication 12 January 2007. This material is declared a work of the U.S. Government and is not subject to copyright protection in the United States. Copies of this paper may be made for personal or internal use, on condition that the copier pay the \$10.00 per-copy fee to the Copyright Clearance Center, Inc., 222 Rosewood Drive, Danvers, MA 01923; include the code 0731-5090/07 \$10.00 in correspondence with the CCC.

\*Military Professor, Department of Mechanical Engineering; rwatkin@usna.edu.

†Distinguished Professor and Director, Spacecraft Research and Design Center; agrawal@nps.edu. Associate Fellow AIAA.

# Report Documentation Page

Form Approved  
OMB No. 0704-0188

Public reporting burden for the collection of information is estimated to average 1 hour per response, including the time for reviewing instructions, searching existing data sources, gathering and maintaining the data needed, and completing and reviewing the collection of information. Send comments regarding this burden estimate or any other aspect of this collection of information, including suggestions for reducing this burden, to Washington Headquarters Services, Directorate for Information Operations and Reports, 1215 Jefferson Davis Highway, Suite 1204, Arlington VA 22202-4302. Respondents should be aware that notwithstanding any other provision of law, no person shall be subject to a penalty for failing to comply with a collection of information if it does not display a currently valid OMB control number.

1. REPORT DATE <b>AUG 2007</b>		2. REPORT TYPE		3. DATES COVERED <b>00-00-2007 to 00-00-2007</b>	
4. TITLE AND SUBTITLE <b>Use of Least Means Squares Filter in Control of Optical Beam Jitter</b>				5a. CONTRACT NUMBER	
				5b. GRANT NUMBER	
				5c. PROGRAM ELEMENT NUMBER	
6. AUTHOR(S)				5d. PROJECT NUMBER	
				5e. TASK NUMBER	
				5f. WORK UNIT NUMBER	
7. PERFORMING ORGANIZATION NAME(S) AND ADDRESS(ES) <b>Naval Postgraduate School,Spacecraft Research and Design Center,Monterey,CA,93943</b>				8. PERFORMING ORGANIZATION REPORT NUMBER	
9. SPONSORING/MONITORING AGENCY NAME(S) AND ADDRESS(ES)				10. SPONSOR/MONITOR'S ACRONYM(S)	
				11. SPONSOR/MONITOR'S REPORT NUMBER(S)	
12. DISTRIBUTION/AVAILABILITY STATEMENT <b>Approved for public release; distribution unlimited</b>					
13. SUPPLEMENTARY NOTES					
14. ABSTRACT					
15. SUBJECT TERMS					
16. SECURITY CLASSIFICATION OF:			17. LIMITATION OF ABSTRACT	18. NUMBER OF PAGES	19a. NAME OF RESPONSIBLE PERSON
a. REPORT <b>unclassified</b>	b. ABSTRACT <b>unclassified</b>	c. THIS PAGE <b>unclassified</b>			

microphone or the accelerometers to the FSM as well as feedback to the FSM using a position sensing detector (PSD) at the target. Glaese et al. [4] conducted similar experiments as McEver and Clark, using acoustically induced jitter and LQG control. These experiments showed a decrease of about one-half of the input disturbance amplitude for broadband disturbances, and almost complete elimination of narrowband disturbances. Adaptive methods such as the least means squares (LMS), broadband feedforward active noise control, model reference, or adaptive lattice filters have also been used to control jitter. Skormin, Tascillo, and Busch developed a computer simulation in 1995 of an airborne to satellite optical link in which the use of a self-tuning regulator (STR) as well as a filtered-X least means squares (FXLMS) controller was used to mitigate the effects of jitter on the optical beam. The simulation shows that adaptive feedforward vibration compensation can be used to minimize induced jitter [1]. In 1997, Skormin and Busch proposed the use of model reference control for jitter reduction. Experiments were conducted using a specially designed high bandwidth FSM and a commercially available low bandwidth FSM. In each case, significant reduction (on the order of 20 dB) in acoustically induced jitter was achieved [5]. Also in 1997, Skormin, Tascillo, and Busch demonstrated the use of a self-tuning regulator in an acoustically induced jitter rejection experiment using FSMs, accelerometers and PSDs. The data showed that the STR was superior to classical feedback control in frequency ranges above about 300 Hz [6].

Adaptive systems require a reference signal to reject the disturbance. The development of this reference signal for the LMS algorithm, and enhancements made to it particular to the laser targeting situation is the subject of this paper. An experimental laser jitter control (LJC) test bed, equipped with fast steering mirrors to correct the beam, has been developed to test various control techniques on vibrational induced jitter. Using this test bed, we will show experimentally that the addition of an adaptive bias signal to the reference signal results in a rapid correction of the bias error by the adaptive controller. The bias effect has been shown previously by Widrow [7], but we have adapted the concept to the laser targeting situation, and provided a means for this bias signal to adapt to changing errors. This paper will first discuss the experimental setup. Following that, the development of the basic control methods used in the experiment, as well as the enhancements made to the reference signal will be explained. Experimental results and conclusions will then be presented.

## II. Experimental Setup

### A. Laser Jitter Control Test Bed

The LJC test bed is located in the Spacecraft Research and Design Center, Optical Relay Mirror Lab, at the Naval Postgraduate School in Monterey, California. The components are mounted on a Newport optical bench, which is used to isolate the components from external vibrations. The idea is to simulate a satellite or vehicle "bus" that houses an optical relay system. The laser beam originates from a source and passes through a disturbance injection fast steering mirror (DFSM). The DFSM corrupts the beam using random or periodic disturbances simulating the disturbances that might occur as a result of the transmitting station or the tip and tilt the beam may suffer as it passes through the atmosphere. A vibration isolation platform is used to mount the relay system, and to isolate the relay system from the optical bench. The relay system platform may be disturbed by a 5 lbf inertial actuator, simulating onboard running equipment such as control moment gyros, reaction wheels, cryocoolers, and so on. The inertial actuator may be located as required on the platform to produce the desired effect. The incoming beam is split and reflected off the platform to a PSD to obtain a reference signal that indicates the onboard and injected disturbances. The PSDs are labeled OT1, for the feedforward detector, and OT2 for the target detector (see Fig. 1). It is recognized that using the PSD labeled OT1 is not a normal means to measure the disturbances onboard the platform used to relay the beam as one would not be able to mount a detector separate from the satellite bus in a practical application. However, this reference PSD may be seen as simulating an onboard inertial measurement unit

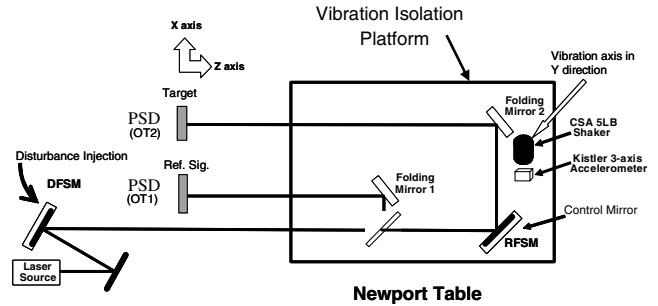


Fig. 1 Laser jitter control test bed schematic.

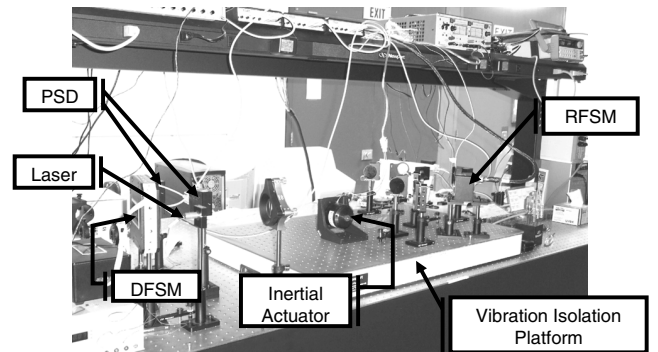


Fig. 2 Laser jitter control test bed.

(IMU), which is normally available in satellites with an optical payload. The IMU provides an accurate inertial position of the platform, which is the same as provided by a PSD mounted on a stable reference plane with respect to the vibrating platform. This setup allows an identical measurement without the added cost of an IMU. A control fast steering mirror (FSM), designated the receive FSM or RFSM, is used to correct the disturbed beam. The corrected beam is then reflected off the platform by a second folding mirror to the target PSD, OT2. A block diagram of the system as well as a picture of the actual setup are shown in Figs. 1 and 2.

### B. Fast Steering Mirrors

The fast steering mirrors are the heart of the LJC. They are used to rapidly and accurately direct the laser beam through the system. The FSMs in the LJC use voice coils to position the mirrors in response to commanded inputs. The LJC uses two different FSMs, one by the Newport Corporation, and one by Baker Adaptive Optics. The Newport FSM is used as the control mirror (RFSM) for all experiments conducted during this research. The mirror comes with its own controller, the FSM-CD100, capable of both open loop and closed loop operation. The controller also provides an output of the mirror's angular position about each of the axis. In these experiments, the controller is configured in the open loop mode, with control inputs provided from the computer control system. The Newport FSM has a control bandwidth of about 800–1000 Hz.

The second FSM used in the LJC is from Baker Adaptive Optics. The Light Force One model is a 1 in. diam DFSM in these experiments. The Baker mirror comes with a small driver for positioning the mirror; however, there is no closed loop option and mirror position is not available. The control bandwidth for the Baker mirror is about 3 kHz.

### C. Position Sensing Detectors

The laser beam optical position sensors, known as position sensing modules or PSMs, have a detection area of  $10 \times 10$  mm. Each duolateral, dual axis PSM requires an amplifier, the OT-301 to output the  $x$  and  $y$  position (in volts) of the centroid of the laser beam spot. The combination of amplifier and detector is called a position sensing detector or PSD. The frequency response of the detectors for the gain

settings normally used is 15 kHz. The minimum resolution of the PSD is 0.5  $\mu\text{m}$ .

#### D. Newport Vibration Isolation Platform and Inertial Actuator

The RFSM, beam splitters, and folding mirrors are mounted on a bench top pneumatic Newport vibration isolation platform. This platform allows the control system actuators and optical path to be vibrated independent of the optical bench. The breadboard, which is self-leveling, rests on four pneumatic isolators. To vibrate the platform at desired frequencies, an inertial actuator is mounted on the vibration isolation platform. This actuator is a CSA model SA-5,

the mirror to the output position of the mirror as measured by the RFSM's integral mirror position measurement system. A first-order system was added to model the optical sensor system:

$$H_d(s) = \frac{1}{Ts + 1} \quad (3)$$

The transfer function  $H_d(s)$  describes the time response between the actual laser beam's position on the surface of the detector and the reported position as measured by the voltage from the detector. The value for  $T$  was determined from the data given for the optical sensors by the manufacturer. The resulting state-space set of equations is given as follows:

$$\begin{bmatrix} \dot{V}_{py} \\ \dot{\theta}_x \\ \ddot{\theta}_x \\ \dot{V}_{px} \\ \dot{\theta}_y \\ \ddot{\theta}_y \end{bmatrix} = \begin{bmatrix} -1/T & 2G_{py}D_m/T & 0 & 0 & 0 & 0 \\ 0 & 0 & 1 & 0 & 0 & 0 \\ 0 & -\omega_x^2 & -2\zeta_x\omega_x & 0 & A_x\omega_x^2 & A_x2\zeta_x\omega_x \\ 0 & 0 & 0 & -1/T & 2G_{px}D_m/T & 0 \\ 0 & 0 & 0 & 0 & 0 & 1 \\ 0 & A_y\omega_y^2 & A_y2\zeta_y\omega_y & 0 & -\omega_y^2 & -2\zeta_y\omega_y \end{bmatrix} \begin{bmatrix} V_{py} \\ \theta_x \\ \dot{\theta}_x \\ V_{px} \\ \theta_y \\ \dot{\theta}_y \end{bmatrix} + \begin{bmatrix} 0 & 0 \\ 0 & 0 \\ G_{mx}\omega_x^2 & 0 \\ 0 & 0 \\ 0 & 0 \\ 0 & G_{my}\omega_y^2 \end{bmatrix} \begin{bmatrix} V_{mx} \\ V_{my} \end{bmatrix} \quad (4)$$

$$\begin{bmatrix} V_{py} \\ V_{px} \end{bmatrix} = \begin{bmatrix} 1 & 0 & 0 & 0 & 0 & 0 \\ 0 & 0 & 0 & -1 & 0 & 0 \end{bmatrix} \begin{bmatrix} V_{py} \\ \theta_x \\ \dot{\theta}_x \\ V_{px} \\ \theta_y \\ \dot{\theta}_y \end{bmatrix} + \begin{bmatrix} 0 & 0 \\ 0 & 0 \\ 0 & 0 \\ 0 & 0 \\ 0 & 0 \\ 0 & 0 \end{bmatrix} \begin{bmatrix} V_{mx} \\ V_{my} \end{bmatrix} \quad (5)$$

capable of delivering a rated force of 5 lbf, in a frequency range of 20 to 1000 Hz.

#### E. Computer Control System

The computer control system is based on MATLAB, version 6.1 release 13 with SIMULINK, and the xPC Targetbox, all from the Mathworks. The main computer for control implementation and experiment supervision is a 2.4 GHz Dell Dimension 8250. The xPC Targetbox is a Pentium III class computer running at 700 MHz and is used to perform digital-to-analog and analog-to-digital conversion. A separate disturbance computer is used to control the inertial actuator and has a 1.4 GHz processor; dSPACE ver 3.3 with ControlDesk ver 2.1.1 is used to interface with the inertial actuator. A sample rate of 2 kHz was used throughout the experiment, which precluded aliasing of any signals of interest.

### III. Mathematical Model

A state-space model of the RFSM/PSD system was used to model the dynamics of the control system. The state-space model is of the form

$$\dot{x} = Ax + Bu, \quad y = Cx + Du \quad (1)$$

A simple second order transfer function of the RFSM (used to correct the beam) about one axis is defined:

$$H_m(s) = \frac{\omega_n^2}{s^2 + 2\zeta\omega_n s + \omega_n^2} \quad (2)$$

where  $\omega_n$  and  $\zeta$  are experimentally determined using the methods in Ogata [8]. The transfer function  $H_m(s)$  relates the ordered position of

The values for  $G$  and  $A$  are determined experimentally and are provided in Table 1, as well as the values used for the other parameters.

A top level view of the FSM provided by Newport Application Note: Opto-Mechanics 2 is shown in Fig. 3.

### IV. Control Methods

#### A. Linear-Quadratic Regulator

The linear-quadratic regulator (LQR) is first developed to investigate how classical control algorithms handle broadband and narrowband disturbances for the control of laser jitter. The system to be controlled, modeled in the preceding section, is used to determine the optimal gains. The LQR requires full state feedback, which, if not available, must be estimated. In this experiment, a Kalman filter is used to estimate the states  $\dot{\theta}_x$  and  $\dot{\theta}_y$ , all others being measured by sensors. The matrix of linear-quadratic optimal gains ( $K$ ) is calculated to minimize the following cost function:

$$J = \int_0^\infty (x^T Q x + u^T R u) dt \quad (6)$$

The control law is

$$u = -Kx \quad (7)$$

The optimum gains are determined using the state-space model of the system, Eqs. (4) and (5). Matrices  $R$  and  $Q$  in Eq. (6) are used to weight the importance of each state and input. For this investigation, the matrices  $R$  and  $Q$  are identity matrices, with the exception of the elements along the diagonal of  $Q$  corresponding to the state  $V_p$  for each axis having a value of  $10^3$ . This value was chosen to provide the

**Table 1 Parameter values**

Name	Variable	Value
PSD voltage, y axis	$V_{py}$	-10 to +10 V
PSD voltage, x axis	$V_{px}$	-10 to +10 V
Rotation about x axis of RFSM	$\theta_x$	$-26.2 \times 10^{-3}$ to $+26.2 \times 10^{-3}$ rad
Rotation about y axis of RFSM	$\theta_y$	$-26.2 \times 10^{-3}$ to $+26.2 \times 10^{-3}$ rad
PSD response time	$T$	$67 \times 10^{-6}$ s
PSD calibration, y axis	$G_{py}$	$2 \times 10^3$ V/m
PSD calibration, x axis	$G_{px}$	$2 \times 10^3$ V/m
Distance from RFSM to target	$D_m$	1.245 m
RFSM damping ratio, x axis	$\zeta_x$	0.90
RFSM damping ratio, y axis	$\zeta_y$	0.90
RFSM natural frequency, x axis	$\omega_x$	5655 rad/s (900 Hz)
RFSM natural frequency, y axis	$\omega_y$	5184 rad/s (825 Hz)
Mirror calibration factor, x axis	$G_{mx}$	$52.4 \times 10^{-3}$ rad/V
Mirror calibration factor, y axis	$G_{my}$	$52.4 \times 10^{-3}$ rad/V
Voltage input to RFSM, x axis	$V_{mx}$	-10 to +10 V
Voltage input to RFSM, y axis	$V_{my}$	-10 to +10 V
Cross-coupling factor, x axis	$A_x$	$-2 \times 10^{-2}$
Cross-coupling factor, y axis	$A_y$	$-2 \times 10^{-2}$

most rapid correction of the error possible while maintaining a robust stable system and was determined experimentally by trial and error.  $K$  was then determined using the MATLAB algorithm  $K = \text{lqr}(A, B, Q, R)$ .

**B. Least Means Squares Algorithm**

The LMS algorithm is one of the most simple yet robust adaptive algorithms. In the LMS algorithm, a reference signal correlated with the disturbance is input to a transversal filter, consisting of  $M$  stages, or taps [9]. The error between the desired beam location at the target and the actual location is fed back to the filter to adjust these taps. In the experiment, the disturbance consists of the vibration of the platform as well as any motion the laser beam may have due to the action of the DFSM. The reference signal is generated by the output of the feedforward PSD (OT1), and the error is generated by the output of the target PSD (OT2), both of which are sampled at a rate of 2 kHz. The output of the transversal filter is used as a control signal to the RFSM. The algorithm uses the method of least squares to find the optimum values for the tap gains.

The reference signal  $x(n)$  is delayed one time step for each of the  $M$  stages, with the exception of the current input, forming a vector of delayed inputs,  $[x(n), x(n-1), \dots, x(n-M+1)]^T$ . The inner product of the vector of tap gains  $w(n)$  and the vector of delayed inputs  $x(n)$  produces the scalar control input  $u(n)$  to the RFSM:

$$u(n) = w^T(n)x(n) \tag{8}$$

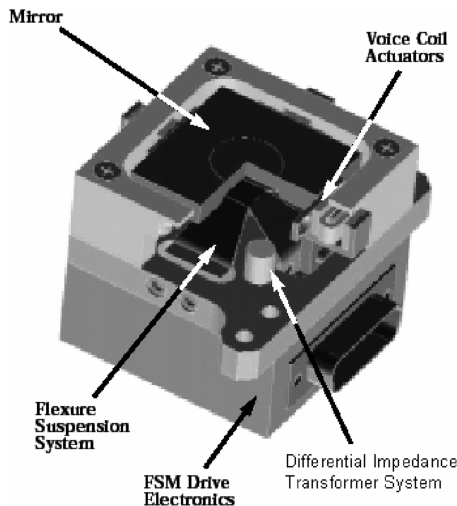


**Fig. 3 Fast steering mirror.**

The desired output  $s(n)$  is that RFSM motion that results in the cancellation of any perturbation in the laser beam caused by the DFSM or the supporting structure and equipment [the disturbance or  $d(n)$ , see Fig. 4]. The error is the difference between the target center and the laser beam's actual position at the target:

$$e(n) = d(n) - s(n) \tag{9}$$

The tap gains are adjusted by means of the update equation developed by Widrow [10]:

$$w(n+1) = w(n) + \mu x(n)e(n) \tag{10}$$

where  $\mu$  is the adaptation step size that controls the stability of the algorithm.

In any practical laser targeting or relay station, there is a secondary path or transfer function that is between the output of the LMS filter and the desired response. In this case, it is the RFSM and related optics used to correct the beam. This secondary path must be modeled in the control algorithm to take into account the delays and other effects that occur to the control signal. To properly make use of the LMS algorithm, a copy of the secondary plant transfer function is placed in the path to the updating algorithm for the weight vector. This is known as the filtered-X LMS (FXLMS) algorithm and was derived by Widrow [7] and Burgess [11]. The block diagram for the use of this algorithm with the LJC test bed is provided in the following: In the FXLMS algorithm, the reference signal is filtered by an estimate of the secondary plant transfer function  $\hat{S}$ , producing the signal  $x'(n) = \hat{S}(n)x(n)$ . This new reference signal is used in the update Eq. (10).

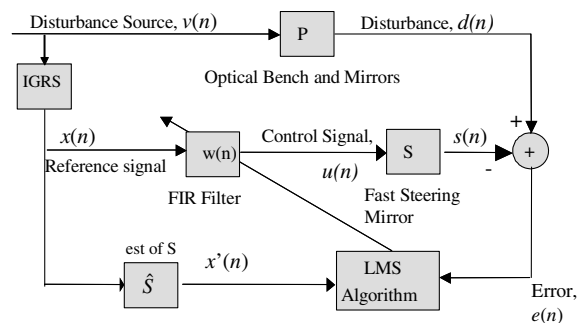


**Fig. 4 Block diagram of the FXLMS control system. The IGRS is a sensor/signal generator that synthesizes a reference signal for the algorithm.**

## V. Correction of Bias Effects Using a Least Means Squares Filter

### A. Effect of Bias on the Least Means Squares Filter

In most laser targeting schemes, a compensator is used to correct the bias error at the target. A second, parallel controller is then used to remove the “noise” in the beam. It has been noted by Widrow that an adaptable bias weight may be used to counteract the effect of “plant drift” in an adaptive inverse modeling situation [12]. This single adjustable weight adapts to remove any bias in the output of the plant. This effect may be analyzed as follows. Referring to Fig. 4 let the disturbance be

$$v(n) = E + F \sin(2\pi f n T_s) \quad (11)$$

Then the desired signal (the signal that must be cancelled) is

$$d(n) = PE + PF \sin(2\pi f n T_s + \phi_o) \quad (12)$$

Now, considering only the bias effect, let the generated reference signal be

$$x(n) = E' + K \sin(2\pi f n T_s) \quad (13)$$

The error then becomes

$$e(n) = d(n) - s(n) = [PE - SWE'] + [PF \sin(2\pi f n T_s + \phi_o) - SWK \sin(2\pi f n T_s + \phi_w + \phi_s)] \quad (14)$$

Thus the proper selection of  $E'$  will result in the cancellation of the dc component of the error. It is also noted that if  $E'$  is zero, the LMS algorithm will be unable to completely cancel the resulting error.  $E'$  should be adaptable, because the bias error may change and because  $W$  is adapting during the process to some quasi-steady state value.

### B. Adaptive Bias Filter

Using a one or two weight LMS filter, the bias in the reference signal is adjusted to remove the dc component of the error signal. An estimate of  $E'$  is used as the reference signal to the adaptive bias filter (ABF); see Fig. 5. The error signal in this case is the mean error, which stops the adaptation once the signal is centered on the target.

## VI. Experimental Results

Five experiments were run on the LJC test bed to explore the capabilities of the FXLMS/ABF controller. The first series of two experiments was run maintaining the vibration isolation platform stable. Two controllers are compared in their ability to remove a bias error as well as two periodic disturbances introduced by the DFSM. In the second series of experiments, the platform is *vibrated* at the same two frequencies used in the first series, and the DFSM is used to provide a random error to the beam. Three controllers are compared

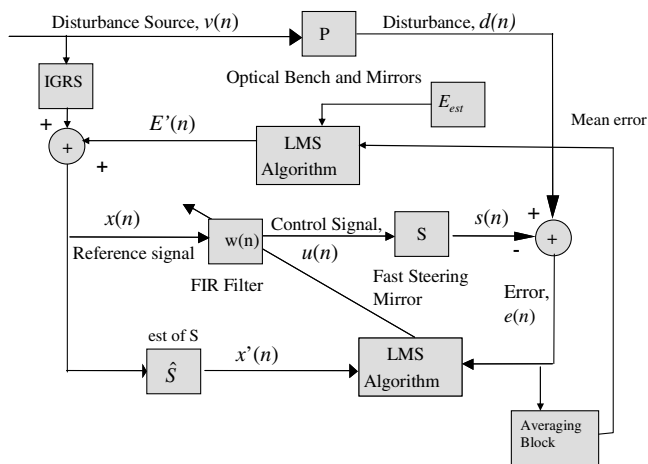


Fig. 5 Block diagram of ABF modification.

in their ability to remove the frequency and random components as well as the bias error; the LQR, FXLMS/ABF, and an LQR + FXLMS/ABF combination.

### A. Bias Effect

The FXLMS controller with the ABF modification was compared with a FXLMS controller with an unbiased reference signal, using a parallel LQR as a compensator. This experiment was run to determine if the addition of bias to the reference signal was better than using a compensator. Random noise was not injected. The LQR compensator was designed using standard MATLAB commands. The mathematical model from Sec. III above was used for the LQR state-space system of equations. An integrator was added to the model to complete the design. A 50 and 87 Hz signal was injected by the DFSM and each controller was used to remove the error in the target signal. The power spectral density (PSD) and mean square error (MSE) for the  $y$  axis of the experiment are provided in Figs. 6 and 7. The  $x$  axis is similar.

From these figures, we see that the addition of the ABF in the LMS controller results in a similar decrease in the power spectral density as using a straight compensator, and that the time constant (the time it takes for the MSE to be reduced by a factor of  $1/e$ ) for the FXLMS/

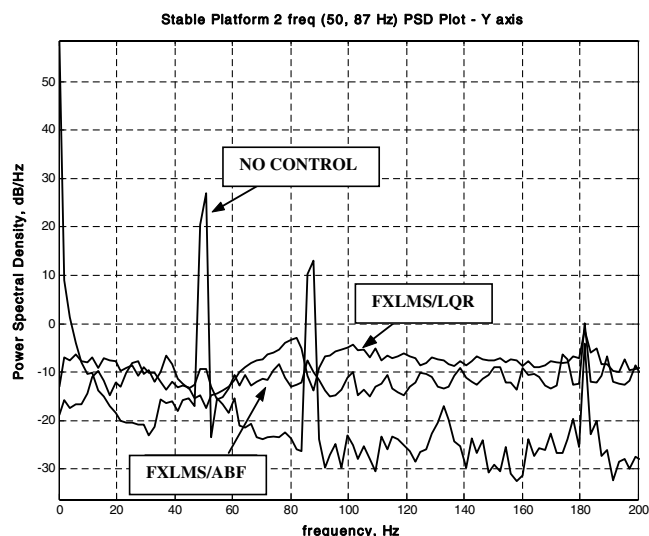


Fig. 6 Power spectral density plot of the stable platform, two frequency bias experiment. The FXLMS controller for both cases was provided a 50 and 87 Hz signal, normalized by the power of the reference signal.

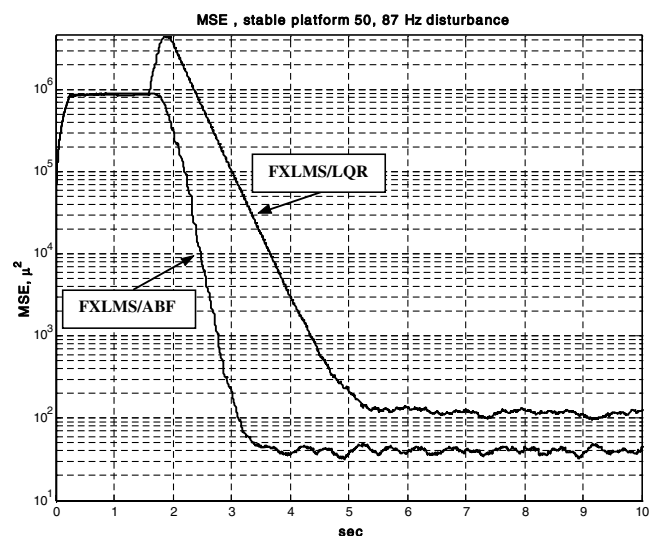


Fig. 7 Mean square error plot of the stable platform, two frequency bias experiment.

ABF controller is less than that for the parallel FXLMS/LQR controller.

## B. Vibrating Platform Results

In this experiment, the platform is vibrated by the inertial actuator at the same two frequencies as in the previous experiment, 50 and 87 Hz. In addition, the DFSM is used to inject a random component of 200 Hz band-limited white noise, to simulate the effect of atmospheric turbulence on the uplink laser beam for a simulated relay station. Because the FXLMS controller uses an internally generated reference signal (IGRS) consisting of the two disturbance frequencies, the controller will not remove the random component. However, by combining the FXLMS controller with the LQR, control of the random component as well as the frequencies added by the inertial actuator may be realized. Additionally, by adding the ABF modification and removing the integrator from the LQR, a faster response to the bias error may also be achieved. A comparison of three experiments using the different control methods is shown in Figs. 8 and 9.

It can be seen from these plots that the use of the LQR + FXLMS/ABF controller results in the best response. The random component is removed and the narrowband frequencies are attenuated. The time constant for the system is dramatically improved over the FXLMS/ABF or LQR controller alone. Table 2 presents the experimental data comparison.

In Table 2, the measure of effectiveness for the jitter is the standard deviation of the laser beam during the last 1 s of a 10 s data run (reported as the controlled beam, standard deviation). The input jitter is the standard deviation of the beam before controller cut on (controller cut on occurs at 1.6 s from the start of data collection). The percent reduction in jitter is the percent reduction in the standard deviation of the beam as compared with the input jitter. The mean value of the beam position is the mean position, in nanometers (nm) over the last 1 s of the data run. It must be noted that the minimum sensitivity of the detector is 500 nm. The total MSE is the combined MSE for both axis, averaged over the last 1 s of the run. As expected, the FXLMS/ABF controller alone does not perform as well as the combination LQR + FXLMS/ABF in the presence of a random disturbance.

## VII. Summary and Conclusions

A unique test bed for the study of the control of jitter in an optical beam has been designed and developed at the Naval Postgraduate School, Spacecraft Research and Design Center. This test bed allows researchers to implement control techniques using fast steering mirrors as actuators to control a disturbed optical beam, whether from the vibration of the support platform or external disturbances to the beam. During this series of experiments, the benefits of providing a properly biased reference signal to a FXLMS controller was investigated. This reference signal was provided by a sensor mounted on a stable platform with respect to the vibrating platform supporting the relay system. This setup simulates what an onboard IMU would provide as a reference signal. A new, adaptive bias filter was demonstrated. This new filter allows rapid zeroing of the optical beam on the target without the use of a compensator, such as a LQR.

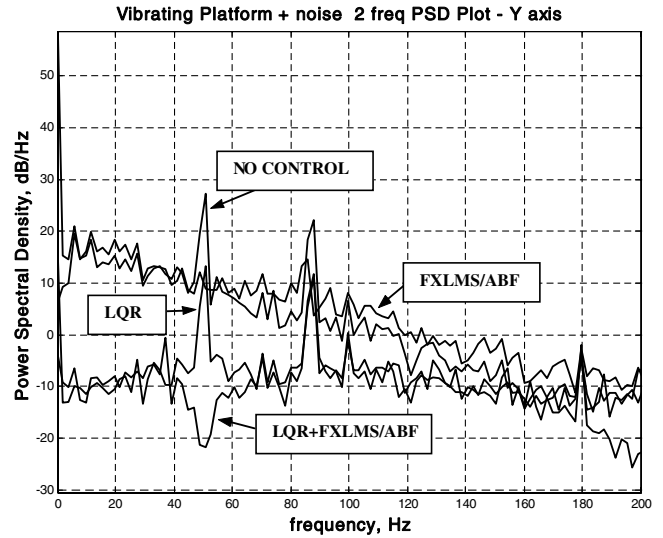


Fig. 8 y axis PSD plot of the two frequency vibrating platform experiment.

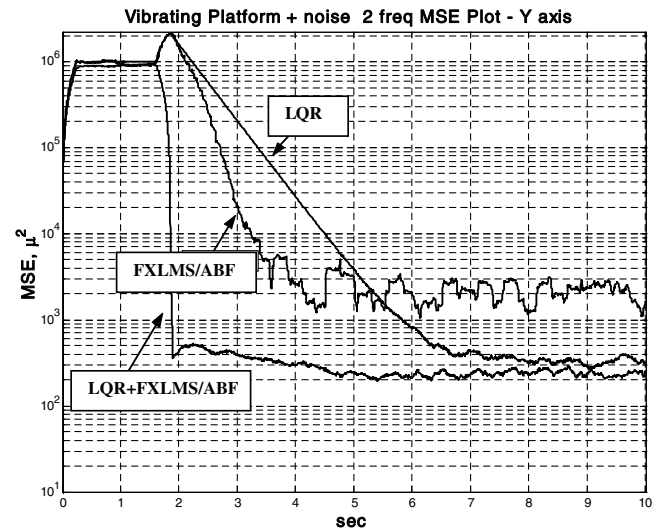


Fig. 9 y axis MSE plot of the two frequency vibrating platform experiment.

It was also shown that for the case of a vibrating support structure for the control system, with a random fluctuating optical beam, a combination of FXLMS/ABF and LQR control could remove the random as well as narrowband components in the disturbed beam. The time constant for the combination controller yielded an improvement of 75% over the LQR control alone. Additionally, the combination LQR + FXLMS/ABF controller reaches the final value for the mean square error of the LQR controller a full 5 s faster than the LQR controller. This may be explained as follows. The

Table 2 Summary of experimental results for the two frequency vibration, random noise case

Controller	LQR		FXLMS		LQR + FXLMS/ABF	
	x axis	y axis	x axis	y axis	x axis	y axis
Control mirror axis	x axis	y axis	x axis	y axis	x axis	y axis
Input jitter, standard deviation, $\mu$	47.7	68.2	47.2	63.9	44.9	65.5
Controlled beam, standard deviation, $\mu$	12.4	18.2	43.3	46.4	12.5	15.3
No. of stages/order	—	—	24	24	24	24
Adaptation rate, m	—	—	0.05	0.05	0.05	0.05
Percent reduction in jitter	73.9	73.3	8.3	27.3	72.2	76.7
Mean value of beam position, nm	165	-763	342	-3063	2	57
dB reduction in PSD of 50 Hz	-14.1	-15.1	-5.0	-16.1	-23.7	-38.7
dB reduction in PSD of 87 Hz	-13.3	-11.2	+1.6	-7.5	-13.1	-10.4
Total MSE at 10 s, $\mu^2$	484.8		4054.9		389.2	
Time constant, s	0.73		0.26		0.18	

FXLMS algorithm will converge faster than the LQR for sinusoidal disturbances, whereas the LQR will be faster than the FXLMS for random disturbances. The combination of FXLMS and LQR will work more effectively and converge faster than either control method alone in the presence of both sinusoidal and random disturbances.

In conclusion, the experimental results demonstrate that the addition of the ABF filter to the FXLMS controller significantly increases the convergence rate of the controller. The FXLMS/ABF control is most effective for a sinusoidal jitter and the LQR control for a random jitter. To achieve a rapid reduction of both sinusoidal and random jitter, a combination of FXLMS/ABF and LQR is more effective than either alone.

### References

- [1] Skormin, V. A., Tascillo, M. A., and Busch, T. E., "Adaptive Jitter Rejection Technique Applicable to Airborne Laser Communication Systems," *Optical Engineering*, Vol. 34, May 1995, p. 1267.
- [2] Hyde, T. T., Ha, K. Q., Johnston, J. D., Howard, J. M., and Mosier, G. E., "Integrated Modeling Activities for the James Webb Space Telescope: Optical Jitter Analysis," *Proceedings of the Society of Photo-Optical Instrumentation Engineers*, Vol. 5487, Society of Photo-Optical Instrumentation Engineers, International Society for Optical Engineering, Bellingham, WA, 2004, pp. 588–599.
- [3] McEver, M. A., and Clark, R. L., "Active Jitter Suppression of Optical Structures," *Proceedings of the Society of Photo-Optical Instrumentation Engineers*, Vol. 4327, Society of Photo-Optical Instrumentation Engineers, International Society for Optical Engineering, Bellingham, WA, 2001, pp. 596–598.
- [4] Glaese, R. M., Anderson, E. H., and Janzen, P. C., "Active Suppression of Acoustically Induced Jitter for the Airborne Laser," *Society of Photo-Optical Instrumentation Engineers Paper 4034-19*, April 2000, pp. 157–162.
- [5] Skormin, V. A., and Busch, T. E., "Experimental Implementation of Model Reference Control for Fine Tracking Mirrors," *Proceedings of the Society of Photo-Optical Instrumentation Engineers* Vol. 2990, Society of Photo-Optical Instrumentation Engineers, International Society for Optical Engineering, Bellingham, WA, Feb. 1997, pp. 183–189.
- [6] Skormin, V. A., Tascillo, M. A., and Busch, T. E., "Demonstration of a Jitter Rejection Technique for Free-Space Laser Communication," *IEEE Transactions on Aerospace and Electronic Systems*, Vol. 33, No. 2, April 1997, pp. 571–574.
- [7] Widrow, B., *Adaptive Signal Processing*, 1st ed., Prentice-Hall, Upper Saddle River, NJ, 1985, pp. 283–285.
- [8] Ogata, K., *Modern Control Engineering*, 4th ed., Prentice-Hall, Upper Saddle River, NJ, 2002, pp. 224–239.
- [9] Haykin, S., *Adaptive Filter Theory*, 3rd ed., Prentice-Hall, Upper Saddle River, NJ, 1996, pp. 366–370.
- [10] Widrow, B., *Adaptive Signal Processing*, 1st ed., Prentice-Hall, Upper Saddle River, NJ, 1985, pp. 99–101.
- [11] Burgess, J. C., "Active Adaptive Sound Control in a Duct: A Computer Simulation," *Journal of the Acoustical Society of America*, Vol. 70, Sept. 1981, pp. 715–726.
- [12] Widrow, B., Shur, D., and Shaffer, S., "On Adaptive Inverse Control," *Proceedings of the 15th Asilomar Conference*, IEEE Signal Processing Society, Pacific Grove, CA, 1981, pp. 185–189.